p. 199.

[6]Donald Long and John Myers, Phys. Rev. 115, 1107 (1959).

[7]J. M. Ziman, *Electrons and Phonons* (Oxford U. P., London, 1960).

[8]E. G. S. Paige, in *Progress in Semiconductors*, edited by Alan F. Gibson and P. E. Burgess (Wiley, New York, 1964), Vol. 8, p. 1.

[9]R. T. Bate, R. D. Baxter, F. J. Reid, and A. C. Beer, J. Phys. Chem. Solids 26, 1205 (1965).

[10]L. Spitzer, Jr. and R. Härm, Phys. Rev. 89, 977 (1953).

[11]J. Appel, Phys. Rev. 122, 1760 (1961).

[12]R. Kubo, J. Phys. Soc. Japan 12, 570 (1957).

[13]S. Fujita, *Introduction to Non-Equilibrium Quantum Statistical Mechanics* (W. B. Saunders, Philadelphia, 1966).

[14]N. H. March, W. H. Young, and S. Sampanthar, *The Many-Body Problem in Quantum Mechanics* (Cambridge U. P., London, 1967).

[15]P. Résibois, Physica 27, 541 (1961).

PHYSICAL REVIEW B VOLUME 4, NUMBER 8 15 OCTOBER 1971

Experimental Investigation of the Band Structure of Graphite

R. F. Willis, B. Feuerbacher, and B. Fitton
Surface Physics Division, European Space Research and Technology Centre, Noordwijk, Holland
(Received 2 April 1971)

Photoemission and secondary electron emission (SEE) measurements have been used to investigate the band structure of graphite. The energy distribution curves obtained from both types of measurements reveal identical features for those transitions to conduction-band states occurring up to 5 eV above the vacuum level. Two minima in the σ_1 conduction band, located at critical points Γ_{3u}^+ and Q_{1u}^+, have been observed at 7.5 and 8.6 eV above the Fermi level. Emission from these final states is observed for $\vec{E} \parallel c$ orientation due to the relaxation of electrons initially excited to P_3^+; this $\vec{E} \parallel c$ transition, which is observed at 14.5 ± 0.5 eV, is in good agreement with the predicted value of 13.5 eV assigned to transitions $P_3^- \rightarrow P_3^+$. The σ-band gap at the Brillouin-zone center has been measured for $\vec{E} \perp c$ to be 11.5 ± 0.1 eV and the separation of the σ bands increases to 15.0 eV at Q in good agreement with the optical reflectivity data. The observation and assignment of interband transitions at higher SEE energies provide additional evidence in support of the two-dimensional band structure proposed by Painter and Ellis. The photoemission measurements give detailed information concerning the nature of the π-band structure at points along the three-dimensional Brillouin-zone face. The splitting of the π bands at P and Q is observed to be 0.8 eV, which gives rise to $\vec{E} \perp c$ transitions at 4.76 and 4.82 eV associated with the saddle-point nature of the π bands at Q, and a value of 0.42 eV for the Slonczewski and Weiss parameter γ_1. The SEE results locate P_3^- below the Fermi level, which provides evidence for electron occupancy at the center of the Brillouin-zone edge in agreement with recent Fermi-surface studies.

I. INTRODUCTION

Graphite is a highly anisotropic crystal of space group C_{6v}^4, with an interlayer spacing (3.37 Å) which is large compared with the interatomic spacing in any single layer (1.42 Å). Consequently most theoretical calculations[1-4] of the electronic band structure have used, as a first approximation, a single two-dimensional layer model which neglects any interaction between successive layers. The electron states may be separated into σ and π bands analogous to the sp^2-hybridized atomic eigenstates, the former referring to states which are even with respect to reflection in the layer plane and the latter to those which are odd. The π bands may be regarded as arising from the overlap of p_z atomic orbitals which are oriented normal to the layer plane. Each energy band in the single-layer approximation splits into two closely spaced states upon including the interaction between successive planes. Since the π bands are related to those atomic orbitals directed normal to the basal plane, it follows that these bands will be particularly sensitive to the interlayer interaction, and the magnitude of the splitting is expected to be greater than that for the σ bands. This splitting of the π bands is responsible for the π valence and conduction bands overlapping at the Brillouin-zone edge which, in turn, determines the complex nature of the Fermi surface and the semimetallic properties of graphite. The π-band structure has, therefore, been the subject of numerous theoretical[5,6] and experimental[7] studies.

Since the interlayer forces are weak, the selection rules determined for interband transitions in the two-dimensional structure remain essentially

the same as those for the three-dimensional Brillouin zone; transitions forbidden in the single-layer approximation are predicted[3,8,9] to be relatively weak in the multilayer crystal. Only transitions between states of the same parity with respect to reflection in the plane are allowed for the electric field vector normal to the c axis, i.e., only $\sigma \rightarrow \sigma$ or $\pi \rightarrow \pi$ transitions occur for $\vec{E} \perp c$. The optical spectra may therefore be divided into π and σ regions, and soft-x-ray emission experiments[10] suggest that there is little overlap between these two regions. Conversely, only $\pi \rightarrow \sigma$ or $\sigma \rightarrow \pi$ transitions are allowed for light polarized such that the electric vector is parallel to the c axis.

Although some success has been achieved in relating the observed physical properties to the various band-structure calculations, particularly concerning the nature of the overlapping π bands at the Fermi surface, considerable discrepancy exists in the assignment of transitions to explain certain features of the optical data.[11] It is pertinent, therefore, to give a brief review of the position with regard to the optical measurements. The results of reflectance measurements with unpolarized light at near normal incidence of Taft and Philipp[12] on natural graphite revealed a narrow peak at approximately 4.5 eV and a broad peak at 14.5 eV in the imaginary part of the dielectric constant normal to the c axis, $\epsilon_{2\perp}$, for light energies between 0.1 and 26 eV. Ergun *et al.*[13] also reported the narrow peak at 4.8 eV. Bassani and Pastori Parravicini[2] adjusted a semiempirical tight-binding calculation to obtain the best fit with this data. The sharp peak at 4.5 eV was attributed to the saddle-point nature of transitions between the π bands about the critical point Q of the two-dimensional Brillouin zone, and the σ-band gap at the zone center Γ was adjusted to 6 eV. The broad peak at 14.5 eV was attributed to transitions between the highest bonding and the lowest antibonding σ states at Q. However, while the agreement between the theoretical and the experimental values for $\epsilon_{2\perp}$ was good for the π bands at Q, the computed peak at 14.5 eV for the σ transitions was much too narrow. Bassani and Pastori Parravicini[2] suggested that increasing the σ-band gap at Γ from 6 to about 10 eV would have the effect of broadening this peak, thus improving the agreement with experiment.

Greenaway *et al.*[9] determined the optical constants of graphite for light polarized in the plane of incidence as a function of the angle of incidence. Both $\epsilon_{\perp}$ and $\epsilon_{\parallel}$ were determined for energies between 2 and 10 eV. A sharp peak in $\epsilon_{2\perp}$ was observed and located at 4.6 eV in agreement with the results of Taft and Philipp.[12] A weak shoulder on this peak at 6 eV was ascribed to $\vec{E} \perp c$ transitions at Γ in agreement with the calculation of Bassani and Pastori Parravicini.[2] Further support for this assignment was proposed by Balzarotti and Grandolfo,[14] who ascribed a weak structure at 6 eV in the thermoreflectance spectrum of graphite to a M_0 critical point at Γ, and proposed that other structure at 5.11 eV was due to a M_1 saddle point for transitions between the π bands at Q. More recent thermoreflectance measurements,[15] however, are not in agreement with this work. Greenaway *et al.*[9] attribute structure in $\epsilon_{2\parallel}$ at 4.8 and 6.0 eV to transitions between the highest σ valence band and the lowest π conduction band on the basis of the fact that, although such transitions are forbidden at Q and P, they are allowed along the two-dimensional Brillouin-zone edge.

No reflectivity measurements have been made for $\vec{E} \parallel c$ above 10 eV. To determine $\epsilon_{\parallel}$ at higher frequencies, Tosatti and Bassani[16] applied a Kramers-Kronig dispersion analysis to the energy-loss data of Zeppenfeld[17] for 60-keV electrons incident at different angles to the c axis of graphite. A strong peak in the imaginary part of the dielectric function was obtained at 11 eV and assigned to a van Hove singularity in the joint density of states between the σ_2 valence band and the π conduction band due to the nearly parallel nature of the bands along the points Γ, Q, and P of the Brillouin zone.[2] Weaker structure at 6 and 16 eV was attributed to transitions from the π valence band to the lowest, σ_1, and the highest, σ_3, conduction bands, respectively, again at general points between Γ, Q, and P.

The above assignments have been made in terms of the two-dimensional band structure calculated by Bassani and Pastori Parravicini.[2] Recently Painter and Ellis[3] have employed an *ab initio* variational calculation to determine the band structure of a single layer of graphite, the general features of which, while in qualitative agreement with those of the earlier calculations, show important quantitative differences between the energies of the bands and the assignment of transitions. Whereas the separation of the π bands at Q is predicted to be 4.6 eV in agreement with the earlier work,[2] other transitions show a marked disagreement. For example, the lowest σ-band gap at Γ is predicted to be 12.2 eV, the separation of the σ bands increasing to 16.3 eV at Q. The weak shoulder on the side of the 4.5-eV peak at 6 eV observed in the reflectance measurements[9] is considered to be a result of the structure of the π bands at Q and not due to $\vec{E} \perp c$ transitions at Γ. The structure at 4.8, 6.0, and 11.0 eV cannot be explained in terms of $\vec{E} \parallel c$ transitions on the basis of this and other band-structure calculations. Painter and Ellis[3] predict $\vec{E} \parallel c$ transitions of 13.5 and 16.5 eV at P and Q, respectively.

Recently, observations have been reported[18] of well-defined maxima in the energy distribution

curve of secondary electrons emitted by graphite which were excited by incident electrons of energy 5–150 eV. The number and the energy location above the Fermi level of these maxima show good agreement with emission from high density-of-states levels located at critical points in the two-dimensional conduction-band structure of Painter and Ellis.[3] In the present paper, we have extended these preliminary measurements employing photoemission as a complementary technique in order to investigate the band structure of graphite over a wide range of excitation energy for both $\vec{E} \parallel c$ and $\vec{E} \perp c$ excitations.

The photoemission (PE) and secondary electron emission (SEE) energy distribution curves reveal identical features for those transitions to conduction-band states occuring up to 5 eV above the vacuum level. In addition, the photoemission measurements provide detailed information concerning the location of initial valence-band states down to several eV below the Fermi level. Direct evidence is provided for the nature of the splitting of the π bands along the face of the three-dimensional Brillouin zone due to interaction between successive layers. The observation and assignment of interband transitions at higher SEE energies provides strong evidence in support of the two-dimensional band structure of Painter and Ellis[3] and the transitions predicted for $\vec{E} \perp c$ and $\vec{E} \parallel c$ over a wide energy range. No 11-eV transition for $\vec{E} \parallel c$ is observed, contrary to the analysis of Tosatti and Bassani.[16]

II. EXPERIMENTAL

Energy distribution measurements of the SEE were obtained using a standard three-grid low-energy electron-diffraction (LEED) Auger system similar to that employed by Scheibner and Tharp[19] in their earlier work on graphite. The hemispherical grid system had an acceptance angle of 100° An improved resolution of approximately 1% was achieved by coupling the second and third grids together and carefully screening the apparatus from stray magnetic fields. The observation of weak maxima in the SEE energy distribution curve was facilitated by modulating both the incident electron beam and the retarding grid voltages simultaneously with a small ac signal (0.1–1.0 eV peak to peak), a technique first reported by Gerlach *et al.*[20] This double- or "cross"-modulation technique prevents distortion of the secondary electron energy distribution which would otherwise occur, particularly at low incident-beam energies, due to the overlapping characteristic energy-loss spectrum. For small amplitudes, the ac component of the collected current is proportional to the first derivative of the total secondary collector current with respect to the retarding voltage V on the coupled grids of the analyzer. The derivative dI/dV vs V curves provide the desired energy distribution of the emitted electrons.[21] The incident-electron-beam current was maintained constant at 0.5 μA and corrections were applied for contact potential differences between the cathode and the specimen, and between the specimen and the analyzer grids.[22]

PE experiments were performed with a 127° electrostatic analyzer, details of which have been published.[23] The sample is illuminated by light at normal incidence to the basal plane, and the analyzer geometry is such that only those electrons which are emitted within a 15° solid angle centered about the normal direction are focused at the exit slit. This fact has not been taken into account in the scaling of the energy distribution curves in electrons per photon per eV. The energy distribution curves were corrected, however, for the transmission and resolution of the analyzer, both of which varied with energy; the resolution varied between 1.3% at 20 eV and 4% at 2 eV. Higher-derivative techniques were used in the detailed analysis of both the PE and the SEE spectra to enhance fine structure present in the curves.

The samples of graphite were highly oriented stress-annealed pyrolytic graphite,[24] $2 \times 0.5 \times 0.1$ cm, which were freshly cleaved prior to insertion into the vacuum system and heated to approximately 1000 °C for several minutes at a background pressure of less than 10^{-9} torr. LEED measurements revealed highly oriented crystallites with the c axes aligned normal to the basal-plane surface.[24] Auger-electron spectroscopy confirmed that the cleaved surface was free of contamination. Measurements were also performed with cleaved single crystals of natural Ticonderoga graphite, which gave essentially identical results except for weaker and poorly resolved structure in the 5–20-eV SEE spectral region. This may be attributable to some degree of rotational disorder with good c-axis alignment between successive layer planes as shown by faint streaking occuring through the hexagonal LEED spot pattern.[25]

III. RESULTS AND DISCUSSION

A. Secondary Electron Emission

The energy distribution curves of the secondary electrons emitted at low primary-beam energies, incident normal to the basal plane, are shown in Fig. 1. The large low-energy peak at approximately 1 eV is attributed to multiple inelastic scattering of excited electrons of no well-defined transition energy.[26] Two strong subsidiary maxima at approximately 3 and 4 eV are superimposed on this secondary electron "cascade" background. Weaker maxima have been resolved in the region 5–20

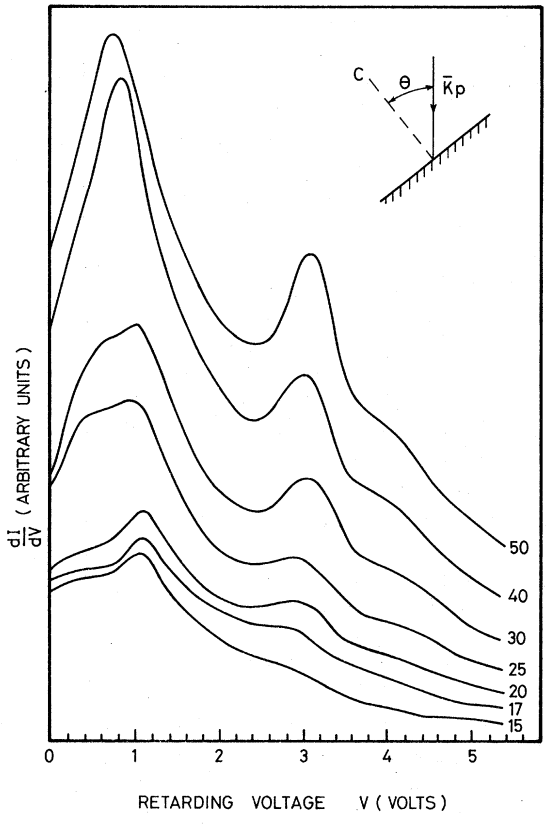

FIG. 1. Energy distribution of secondary electrons emitted from graphite by electrons of energy 15–50 eV incident normal to the basal plane, $\theta = 0°$. Incident-beam energies are shown alongside the appropriate curve.

eV,[18] the relative intensity variations of which are shown by the spectra in Figs. 2(a) and 2(b) for incident-electron energies of 29–45 V. This fine structure has been enhanced by ten times sensitivity compared to that shown in Fig. 1. The relative intensities of these peaks in the SEE spectrum of graphite remain independent of increasing beam energy above 45 eV; the "cascade" background shows a linear increase in intensity.[27] Their intensities change abruptly below 40-eV primary-beam energy, however, as shown in Figs. 2(a) and 2(b). As a consequence of the diminished intensities of the neighboring structure, another weak maximum was observed at 8.5 eV for primary-beam energies below 33 eV [Fig. 2(b)]. For primary-beam energies between 20 and 30 eV, the fine structure observed in the region 5–20 eV was very weak and higher-derivative techniques were required to resolve the various peaks.

The combined energy width of the valence and conduction bands of graphite is predicted[1–3] to be of the order of 40–50 eV, the valence bandwidth being 15–20 eV.[10] Incident-electron-beam energies of 40 eV and higher, therefore, would be expected to populate most final states in the conduction band due to both direct and indirect interband transitions.[28] Both the number, and energetic position, of the above maxima are in close agreement with those critical points above the vacuum level in the calculated conduction band, as shown in Table I, using the notation of Ref. 3. It has therefore been proposed[18] that the structure observed in the SEE spectrum of graphite is due to electrons emitted from high density-of-states levels located at these critical points. The photoemission measurements endorse the view that the relative intensities of the maxima will not necessarily reflect the true density-of-states function, since electrons initially excited to higher states in a conduction band may populate lower band minima in the same band through relaxation processes involving inelastic electron-electron and electron-phonon scattering, and also Auger processes, prior to emission from these points.

The peaks appearing at 3, 4, 10, and 14.5 eV occur for both 0° and 40° angles of incidence θ of the primary beam relative to the c axis, whereas the peaks at 7.5, 8.5, 12, and 17.5 eV are only observed when the crystal is rotated to give oblique incidence [compare the dashed curve shown in Fig. 2(b)]. The selection rules for allowed *optically* excited interband transitions in the two-dimensional approximation[2] predict both $\vec{E} \perp c$ and $\vec{E} \parallel c$ transitions to states at P_3^+ and Q_{1g}^+, while only $\vec{E} \perp c$ transitions are allowed to states at Γ_{2g}^-, Γ_{1u}^+, Q_{2u}^+, and P_1^+. The variation of the SEE peak intensities with θ suggests that for the incident electron beam parallel to the c axis, direct interband transitions are excited by an electric field vector which is also parallel to the c axis. Rotating the crystal through 40° introduces a $\vec{E} \perp c$ component. Final states at the critical points Γ_{2g}^-, Γ_{1u}^+, Q_{2u}^+, and P_1^+ are populated by $\vec{E} \perp c$ transitions while those at Γ_{3u}^+, Q_{1u}^+, P_3^+, and Q_{1g}^+ occur for $\vec{E} \parallel c$, or $\vec{E} \parallel c$ and $\vec{E} \perp c$ transitions (grazing incidence studies, $\theta = 90°$, were not possible with the present system).

The observations are in agreement with the selection rules for optically excited direct transitions, with the exception of transitions to Γ_{3u}^+ and Q_{1u}^+, corresponding to the strong peaks at 3 and 4 eV, respectively, which are predicted for $\vec{E} \perp c$ only. The variation in intensity of these peaks with incident angle θ (taken as the peak-to-peak height of the derivative of the energy distribution curve, Fig. 1) is shown for incident-electron-beam energies near the threshold energies for the excitations in Fig. 3. The intensity of the 4-eV peak has been normalized to be of the same order of magnitude as the 3-eV peak for clarity. At an angle of incidence of 40°, the threshold energy for the 3-eV peak is approximately 11.5 eV and that

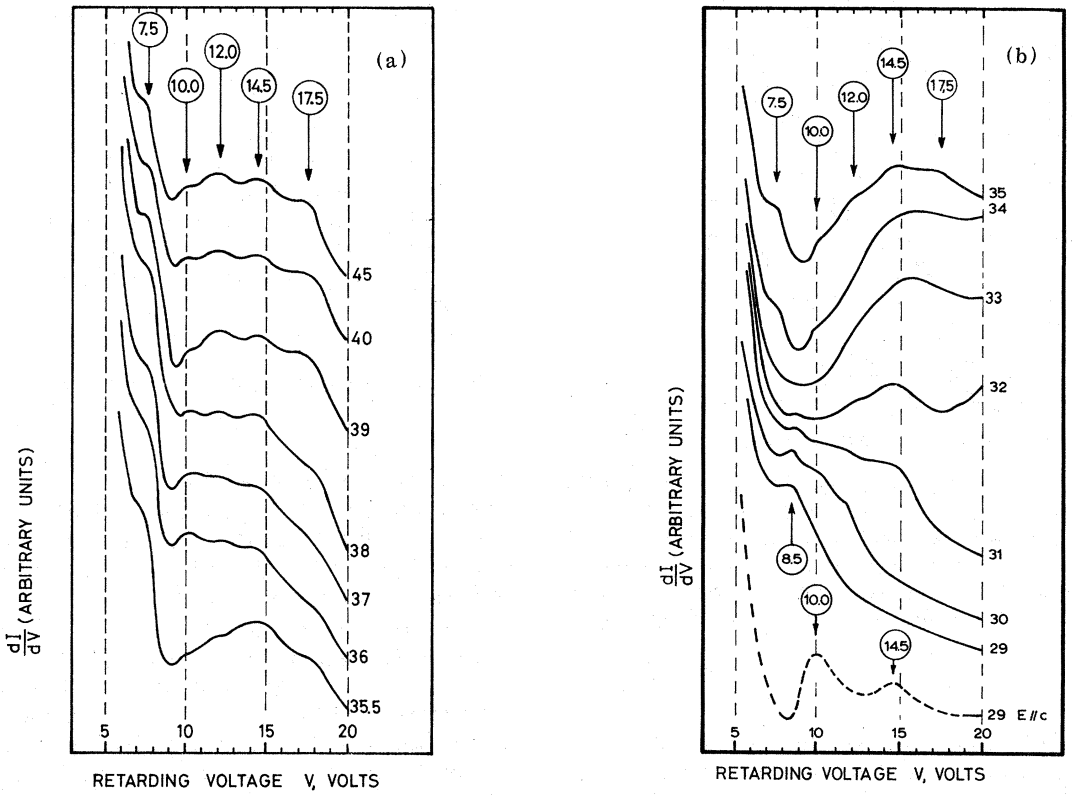

FIG. 2. Energy distribution curves showing the variation in intensity of the peak structure appearing in the 5–20-eV region of the SEE spectrum (a) for incident-beam energies of 35.5–45 eV and (b) for incident-beam energies of 29–35 eV. The full curves were recorded for an angle of incidence $\theta = 40°$. The dashed curve, part (b), was obtained by rotating the crystal to normal incidence, $\theta = 0°$, the peaks appearing at 10 and 14.5 eV being associated with $E \parallel c$ interband transitions. The various curves corresponding to different beam energies are shifted vertically for clarity.

for the 4-eV peak occurs 1 eV higher. The intensity of both peaks increases up to 15 eV, at which point both transitions first appear simultaneously for normal incidence excitation, $\theta = 0°$.

Assuming that for normal incidence only $\vec{E} \parallel c$ transitions are excited, while for $\theta = 40°$, both $\vec{E} \parallel c$ and $\vec{E} \perp c$ excitations are possible, the above results are in very good agreement with those transitions predicted by the analysis of Painter and Ellis[3] for the two-dimensional crystal band structure, reproduced in Fig. 4. For the sake of illustration, the three-dimensional Brillouin zone of graphite is shown in Fig. 5 with the notation of Ref. 3. This model predicts two minima at Γ_{3u}^{+} and Q_{1u}^{+} in the lowest σ conduction band, the positions of which are in close agreement with the observed peaks (Table I). The σ-band gap at Γ is 12.2 eV and the predicted $\vec{E} \perp c$ transition is in good agreement with the threshold of the interband transition of energy 11.5 eV observed for the 3-eV peak (Fig. 3). The 4-eV peak appears at an incident-electron energy of approximately 12.5 eV in agreement with Q_{1u}^{+} appearing 1 eV higher, at an energy where the electrons excited from Γ_{3g}^{+} can relax into this second minimum. The intensity of both peaks increases up to 15 eV ($\theta = 40°$, Fig. 3), corresponding to the fact that the σ bands are flat and parallel at the points Q_{2g}^{+} and Q_{1u}^{+}.

This interpretation of the results is also in agreement with the optical data of Taft and Philipp,[12] which show a strong transition beginning at about 11 eV for $\vec{E} \perp c$, the oscillator strength increasing up to approximately 14 eV at Q. The intensities of the 3- and 4-eV SEE peaks level off at this energy due to the increased dispersion of the σ bands between Q and P, which results in a decrease in the oscillator strength at higher transition energies. The Kramers-Kronig dispersion analysis performed by Tosatti and Bassani on Zeppenfeld's data ascribed a strong energy loss at 11 eV to be an $\vec{E} \parallel c$ transition. A recent determination of the optical constants of graphite from reflectivity studies with light polarized $\vec{E} \parallel c$ using synchrotron radiation[29] does not show any strong peak in $\epsilon_2 \parallel c$ at 11 eV, contrary to this analysis. However, these reflectivity measurements are in good agreement with the present results. A broad peak in $\epsilon_2 \parallel c$ centered about 15 eV is indicative of $\vec{E} \parallel c$

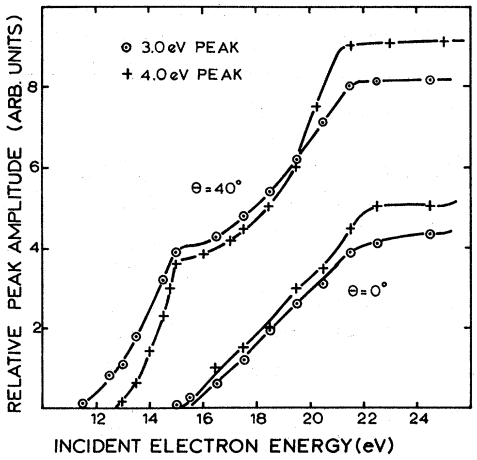

FIG. 3. Variation in relative peak amplitude (taken to be the peak-to-peak height of the derivative of the energy distribution curve) with incident electron energy for peaks appearing at approximately 3 and 4 eV in the SEE spectrum. The incident electron energy was corrected for the contact potential difference between the cathode and the specimen.

transitions, which agrees with the threshold energy for the appearance of the 3- and 4-eV peaks for normal incidence ($\theta = 0°$, Fig. 3). We assign this transition threshold to be a $\pi \rightarrow \sigma$ transition, P_3^- to P_3^+, which is predicted to be 13.5 eV in Fig. 4. The observed increase in intensity of the peaks with increasing excitation energy is interpreted as being due to the relaxation of electrons, initially excited to states at P_3^+, down into the two minima at critical points Γ_{3u}^+ and Q_{1u}^+ in the σ_1 conduction band.

It was not possible to plot the intensity variation of the fine structure occurring in the 5–20-eV region of the SEE spectrum. However, in Table II, the minimum incident-electron-beam energies

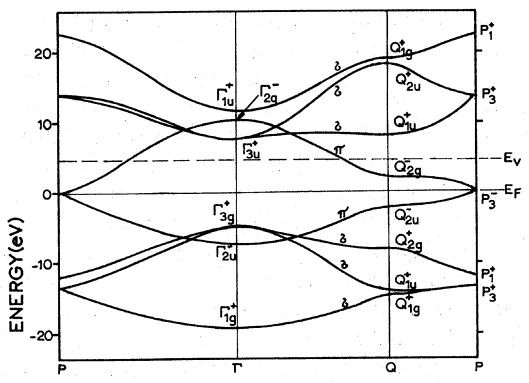

FIG. 4. Energy-band structure of a single two-dimensional layer of graphite calculated by Painter and Ellis, Ref. 3.

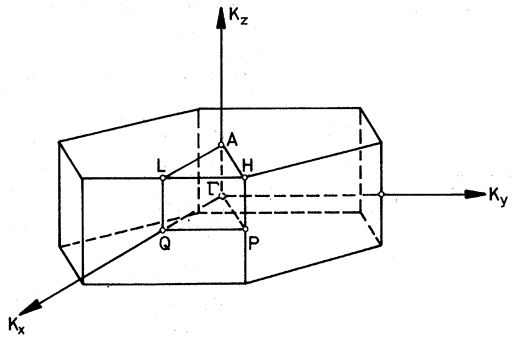

FIG. 5. Three-dimensional Brillouin zone of graphite.

below which these weak SEE peaks were no longer observed, and the energies at which sharp changes in the relative intensities of the various maxima occured for $\theta = 0°$ and $\theta = 40°$ (cf. Fig. 2), are compared with the $\vec{E} \perp c$ and $\vec{E} \parallel c$ optical transition energies predicted by Fig. 4. The intensities of the individual maxima change with excitation energy in such a manner as to make unambiguous assignments difficult. In some cases, the peak intensities are the result of direct transitions from several valence-band states and, for $\theta = 40°$, both $\vec{E} \parallel c$ and $\vec{E} \perp c$ transitions can occur simultaneously. Also, as Bauer[28] has pointed out, indirect transitions can be excited in addition to direct transitions due to the momentum transferred to the excited electron by the incident low-energy electrons. These indirect processes will tend to smear out any structure due to direct transitions. Nevertheless, with these limitations in mind, the tentative assignments in Table II show good agreement with those predicted[3] at critical points Γ, Q, and P. It was not possible to resolve the very weak struc-

TABLE I. Comparison between the energies of maxima observed in the SEE spectrum and critical points in the theoretical conduction-band structure (Ref. 3) at which high densities of final states would be expected.

Conduction-band state[a]	Energy with respect to Fermi level (eV) Theoretical[a]	Observed[b]
Γ_{3u}^+	7.5	7.7 ± 0.5
Q_{1u}^+	8.0	8.7 ± 0.5
Γ_{2g}^-	10.5	12.2 ± 0.5
Γ_{1u}^+	11.5	13.2 ± 0.5
P_3^+	13.5	14.7 ± 0.5
Q_{2u}^+	17.5	16.7 ± 0.5
Q_{1g}^+	18.5	19.2 ± 0.5
P_1^+	22.0	22.2 ± 0.5

[a]See Ref. 3.

[b]Work function of graphite taken to be 4.7 eV. Data corrected for contact potential differences between specimen and analyzer grids.

TABLE II. Comparison between the threshold energies of transitions associated with maxima observed in both the SEE and PE spectra and transitions predicted on the basis of a recent theoretical band structure (Ref. 3) for light polarized parallel or normal to the c axis.

Conduction-band state	Allowed [a] transition	Optical-selection rule	Transition energy (eV) Theor.	Obs.	Spectra
Q_{2g}^-	$Q_{2u}^- \rightarrow Q_{2g}^-$	$\vec{E} \perp c$	4.7	4.7±0.1	PE
	$Q_{1u}^+ \rightarrow Q_{2g}^-$	$\vec{E} \parallel c$	16.0	• • •	
Γ_{3u}^+	$\Gamma_{3g}^- \rightarrow \Gamma_{3u}^+$	$\vec{E} \perp c$	12.2	11.5±0.1	SEE/PE
Q_{1u}^+	$Q_{2g}^+ \rightarrow Q_{1u}^+$	$\vec{E} \perp c$	16.0	15.0±0.5	PE(yield)
	$Q_{1g}^+ \rightarrow Q_{1u}^+$	$\vec{E} \perp c$	23.0	25.0±1.0	SEE
Γ_{2g}^-	$\Gamma_{2u}^- \rightarrow \Gamma_{2g}^-$	$\vec{E} \perp c$	17.5	<20.0	SEE
Γ_{1u}^+	$\Gamma_{1u}^+ \rightarrow \Gamma_{1u}^+$	$\vec{E} \perp c$	16.5	<20.0	SEE
				(17.0±0.5)	(PE)
P_3^+	$P_3^- \rightarrow P_3^+$	$\vec{E} \parallel c$	13.5	14.5±0.5	SEE
	$P_1^+ \rightarrow P_3^+$	$\vec{E} \perp c$	25.0	25.0± 2.0	SEE
	$P_3^+ \rightarrow P_3^+$	$\vec{E} \parallel c$	26.5	26.0± 2.0	SEE
Q_{2u}^+	$Q_{2g}^+ \rightarrow Q_{2u}^+$	$\vec{E} \perp c$	26.0	25.0±2.0	SEE
	$Q_{1g}^+ \rightarrow Q_{2u}^+$	$\vec{E} \perp c$	32.5	33.0±2.0	SEE
Q_{1g}^+	$Q_{1u}^+ \rightarrow Q_{1g}^+$	$\vec{E} \perp c$	32.5	31.0±2.0	SEE
	$Q_{2u}^- \rightarrow Q_{1g}^+$	$\vec{E} \parallel c$	21.0	22.0±2.0	SEE
P_1^+	$P_3^+ \rightarrow P_1^+$	$\vec{E} \perp c$	35.0	34.0±2.0	SEE

[a] Allowed optical transitions with light polarized $\parallel$ or $\perp$ to the c axis in the two-dimensional layer structure at symmetry points Γ, Q, and P (Ref. 3).

ture occurring at 7.5 and 8.5 eV in the SEE spectrum, corresponding to final states at Γ_{2g}^- and Γ_{1u}^+, respectively, for primary-beam energies below 20 eV due to interference from inelastically scattered primary electrons which could not be suppressed completely at these very low energies. However, it will be shown that the PE measurements indicate that the top of the σ valence band, Γ_{3g}^+, is located at approximately 4 eV below the Fermi level, which gives a value for the transition $\Gamma_{3g}^+ \rightarrow \Gamma_{1u}^+$ of 17.0± 0.5 eV for $E \perp c$ in good agreement with the theoretical value. The agreement between the SEE and the PE results at lower excitation energies is also good.

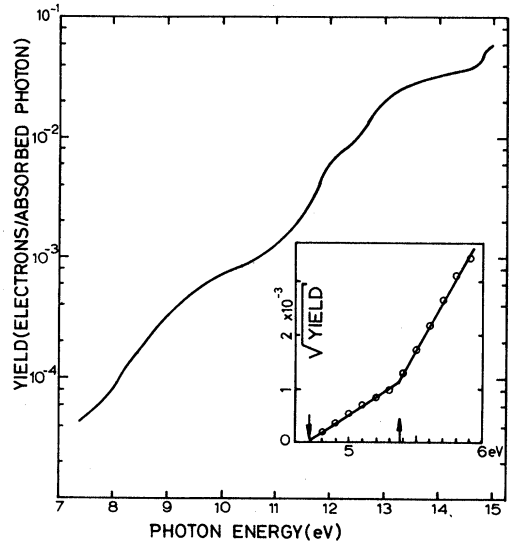

FIG. 6. Variation of photoelectron yield with photon energy in the range 7–15 eV. The Fowler plot gives a work function Φ of 4.7 eV for the pyrolytic graphite specimen.

B. Photoemission

In the PE measurements, the light was incident normal to the basal plane of graphite so that only transitions $\vec{E} \perp c$ were excited. The absolute photoelectric yield, in electrons per absorbed photon, is shown in Fig. 6. The Fowler plot (inset) extrapolates to zero yield at 4.7 eV, to give the value of the work function Φ of the pyrolytic graphite specimens. The inflexion in the curve at 5.4 eV is interpreted as being due to a high density-of-states level located at about 0.7 eV below the Fermi level, transitions from which produce an increase in the yield. Such a conclusion would be consistent with that of Taft and Apker[30] and soft-x-ray emission data,[10] which showed the density of states to be relatively small at the Fermi level and rising to a value several-fold higher 1 eV or so below. Further confirmation is provided by the PE energy

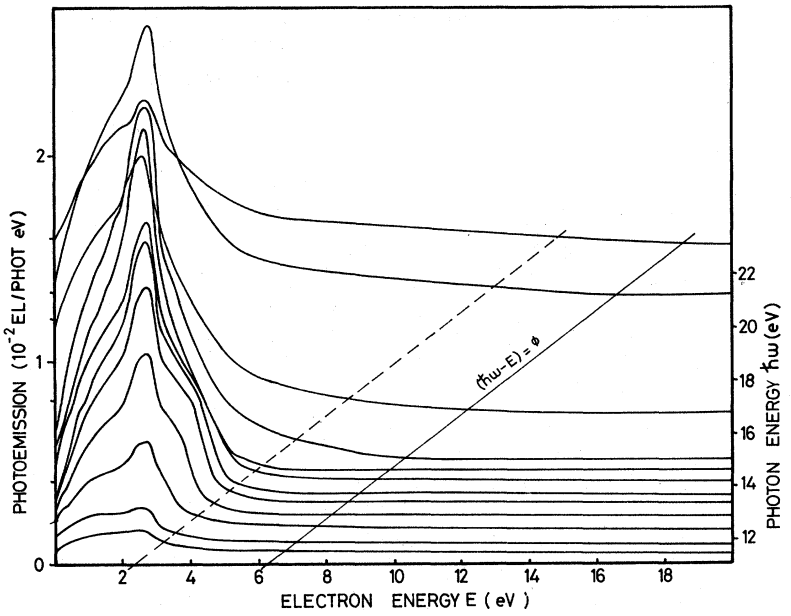

FIG. 7. Energy distribution curves of photoemitted electrons for photon energies of 11 to 23 eV; each curve is shifted vertically according to the photon energy shown at the right-hand side of the diagram. The position of the peaks relative to the vacuum level is shown by the abscissa scale. The full line, $(\hbar\omega - E) = \Phi$, represents the energy of electrons emitted from the Fermi level.

distribution measurements shown later which assign this high density of states to the level P_1^-, which arises due to the lifting of degeneracy of the π bands at the Fermi level P_3^-, in the three-dimensional band structure.

The absolute calibration of the photoelectric yield was achieved by transferring the calibration from a standard lamp[31] to four wavelengths between 1608 and 584 Å using a Reeder thermopile. Interpolation between these points was performed with a photomultiplier coated with sodium salicylate. The yield curve was used to scale the photoelectron energy distribution curves in terms of electrons per photon per eV. Figure 7 shows a set of such curves measured for photon energies between 11.5 and 23.2 eV. Each curve is shifted vertically according to their photon energies given by the right-hand scale. The curves have been superimposed such that the position of those electrons emitted from the Fermi level is marked by the full line, $\hbar\omega - E = \Phi$. On the abscissa scale, the kinetic energies of the emitted photoelectrons increase towards the right, the zero point corresponding to the vacuum level.

The PE spectra may be regarded as being composed of two regions separated by the broken line in Fig. 7. While there is some question of the propriety of dividing the optical spectra of graphite into regions characterized by π-π and σ-σ electron transitions, band-structure calculations[1-4] show that the σ-π valence-band overlap is only of the order of 2 or 3 eV, which suggests that this separation is justified. Hence, the rough separation

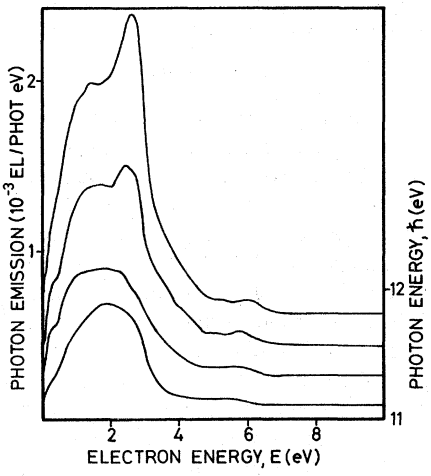

FIG. 8. Energy distribution curves of photoemitted electrons for photon energies of 11 to 12 eV showing the threshold energy for the growth of a peak at approximately 3 eV.

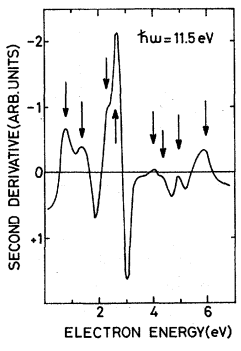

FIG. 9. Derivative of the energy distribution curve of photoemitted electrons for 11.5-eV incident photon energy.

of the PE spectra into two regions in Fig. 7 serves to locate the top of the σ valence band about 4 eV below the Fermi level, which is in reasonable agreement with the value of 5.2 eV quoted by Painter and Ellis.[3] A relatively low number of electrons are photoemitted on the high-electron-energy side of this line compared with the marked increase occuring at lower electron energies. The low number of electrons observed in this region (the energy distribution of which is shown in more detail in Fig. 6) is attributed to mainly indirect processes occurring between the π bands. Direct transitions between the π bands are forbidden at Γ but allowed in the region of Q for $\vec{E} \perp c$. The strong direct transition $Q_{2u}^{-} \rightarrow Q_{2g}^{-}$ associated with the peak at approximately 4.5 eV in the reflectance measurements [12] is not observed in the PE measurements, however, since the final state is situated below the vacuum level (Fig. 4). The increase in the number of electrons observed at lower electron energies may be associated with the onset of transitions between the σ bands centered about Γ, for which allowed $E \perp c$ transitions are predicted.

The main feature of the energy distribution curves in Fig. 7 is the strong peak occurring at 2.8 eV above the vacuum level, i.e., 7.5 eV above the Fermi level, which increases in intensity strongly for photon energies greater than 11.5 eV. The onset of this transition is shown in greater detail in Fig. 8 for photon energies of 11.1–11.8 eV; Bauer and Spicer[32] have recently reported the observation of a similar peak at 7.5 eV above the Fermi level for PE from Aquadag. A second peak, occurring as a shoulder on the above transition, appears at 3.9-eV electron energy for excitation energies above 12.5 eV. The positions of these two structures were observed with greater accuracy using higher-derivative spectra and found to remain at constant electron energies for photon energies up to 23 eV, in agreement with the earlier observations on the SEE structure at approximately 3 and 4 eV.

Fine structure appearing in the above PE spectra may be resolved using higher-derivative techniques.[33,34] For example, Fig. 9 shows the second derivative of the PE energy distribution curve for 11.5-eV photon energy. For clarity, the curve is inverted such that a peak in the energy distribution curve is represented by a peak rather than a minimum. The derivation was performed by a computer using the stored digital information of the 11.5-eV curve and a derivation grid of 0.3 eV.[23] In Fig. 10, the energy values of the peaks observed in the derivative spectra for photon energies from 7.7 to 15 eV are plotted against photon energy. Peaks due to electrons excited to, or from, flat regions of bands, appear on straight lines as well as those peaks due to indirect transitions from, or to, high density-of-states levels. Final states are located on the horizontal lines and initial states lie on lines parallel to, and below, the dashed line at 45°, which represents those electrons emitted from the Fermi level. Peaks on curved, or on straight lines at angles other than 45°, are characteristic of direct transitions. The diagram represents, therefore, the movement of peaks with photon energy observed in the PE energy distribution curves. The particular spectral features appearing in the second-derivative curve, Fig. 9, are located in Fig. 10 at points where these lines intercept the fine line drawn at 11.5-eV photon energy.

Three structures appear to be independent of photon energy in Fig. 10. A large peak (line 6) situated at approximately 0.8 eV above the vacuum level is due to multiple-scattered electrons.[21] The 2.8- and 3.9-eV peaks, referred to in Figs. 7 and 8, are located with respect to the electron-energy ordinate by the horizontal lines 7 and 8, respectively. The 2.8-eV peak, which has been assigned to a minimum in the σ_1 conduction band at Γ_{3u}^{+}, 7.5 eV above the Fermi level, can still be seen as a relatively weak peak in the second-derivative curve at photon energies below 11.5 eV, i.e., below the σ band gap for direct $\vec{E} \perp c$ transitions. This is indicative of indirect transitions also occurring about Γ. Above 11.5-eV photon energy, electrons are excited to higher levels, some of which relax into this σ conduction-band minimum.

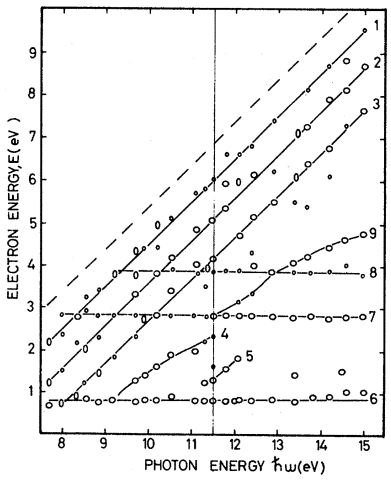

FIG. 10. Electron-energy diagram showing the movement of different maxima appearing in the derivative of the energy distribution curves of photoemitted electrons for incident photon energies between 7.7 and 15 eV. Final states are located on the horizontal lines and initial states lie on lines parallel to, and below, the dashed line at 45° which represents those electrons emitted from the Fermi level; peaks on curved, or on straight lines at angles other than 45°, are characteristic of direct transitions.

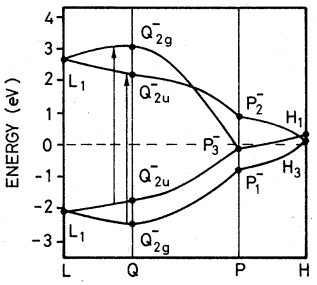

FIG. 11. Band structure of graphite for points located on the vertical face of the three-dimensional Brillouin zone according to Refs. 8 and 9. The separation of the bands has been adjusted to fit the photoemission data in Fig. 10 and the thermoreflectance data of Ref. 15.

Similarly, the 3.9-eV peak (line 8) occurring approximately 1 eV higher in electron energy, shows a marked increase in intensity for photon energies above 12.5 eV, in agreement with the SEE results. The curved line 9 is characteristic of direct transitions probably between the σ bands at general points in the Brillouin zone around Γ.

These results are in agreement with the optical-reflectivity investigations.[12] The interband energy surface at the Brillouin-zone center Γ is small so that the onset of direct transitions between the σ bands is not expected to contribute strongly to $\epsilon_{2\perp}$. The observed increase in $\epsilon_{2\perp}$ between 11 and 15 eV is a consequence of the dispersion of the σ bands between Γ and Q, and the increasing surface exposed in k space over which direct interband transitions can occur in this energy range. $\vec{E} \perp c$ transitions are allowed at general points along $\Gamma_{3u}^+ - Q_{1u}^+ - P_3^+$ and are strongest around Q where the σ conduction and valence bands are nearly parallel, Fig. 4. A marked increase in the 3.9-eV peak at a photon energy of approximately 15 eV, due to the onset of the predicted $Q_{2g}^+ \rightarrow Q_{1u}^+$ saddle-point transitions, is not observed directly in the PE or the SEE spectra since electrons excited to this minimum in the σ_1 conduction band are able to relax into the energetically lower minimum at Γ_{3u}^+. Therefore, the relative population of the final states associated with these two minima in the σ_1 conduction band is observed to remain constant with increasing excitation energy. A further indication of these strong direct σ-σ interband transitions occurring between Γ and Q is given by the sharp increases in the yield curve (Fig. 6) at approximately 11 and 14.5 eV. The observed decrease[12] of $\epsilon_{2\perp}$ above 15 eV may be explained in terms of the large dispersion of the σ bands between Q and P in the band structure shown in Fig. 4.

The 45° lines 1, 2, and 3 in Fig. 10 locate initial states -0.8, -1.8, and -2.6 eV below the Fermi level, and are a result of the splitting of the π valence bands due to interlayer interaction. This interaction between layers introduces a four-atom unit cell in place of the two-atom unit cell used in the two-dimensional approximation. As a consequence, each band in the single-layer band structure (Fig. 4) splits into two closely spaced bands in order to accommodate the eight extra valence electrons per unit cell. Along directions $LQPH$ of the Brillouin zone, Fig. 5, the states Q_{2g}^- and Q_{2u}^- each split into states Q_{2u}^-, Q_{2g}^- and Q_{2g}^-, Q_{2u}^-, respectively, and the point P_3^- in the two-dimensional Brillouin zone is split into states P_2^-, P_3^-, and P_1^-; the P_3^- state being doubly degenerate along the Brillouin-zone edge. The structure of the π bands along the vertical face of the three-dimensional Brillouin zone has been determined by Doni and Pastori Parravicini[8] and Greenaway *et al.*,[9] details of which are reproduced in Fig. 11. The separation of the bands has been adjusted to fit the PE data contained in Fig. 10, and the thermoreflectance data of Ref. 15.

The state -0.8 eV below the Fermi level has been attributed[35] to P_1^- and explains the increase in the density of initial states deduced earlier from the Fowler plot, Fig. 6. The two states at -1.8 and -2.6 eV are assigned to the valence states Q_{2u}^- and Q_{2g}^-, respectively, which gives a π-band splitting of 0.8 eV at Q. The optical experiments[9,11,12] have not resolved this splitting since the allowed transitions between even and odd states at Q (i.e., $Q_{2u}^- \rightarrow Q_{2g}^-$ and $Q_{2g}^- \rightarrow Q_{2u}^-$), differ by less than 0.1 eV. Recent thermoreflectance measurements[15] have resolved these two transitions, however, showing transition energies of 4.76 and 4.82 eV. The splitting of the π bands at P is observed to be the same as that at Q as predicted.[8,9]

The movement of peaks described by the curved line (4) in Fig. 10, which occurs for photon energies in the range 9–11 eV, is due to direct π-π transitions at general points along the bands between Q and Γ. This assignment is further supported by the fact that another set of direct transitions is located by curve 5 occurring for photon energies between 11.3 and 12.1 eV, associated with a peak occurring approximately 0.8 eV lower in electron energy, which is attributed to transitions from the lower of the two split π states.

The Slonczewski-Weiss model[5] is commonly used to describe details of the π energy-band structure along the Brillouin-zone edge in terms of certain overlap parameters γ_0, γ_1, γ_2, γ_3, γ_4, and Δ, values of which have been determined experimentally from Fermi-surface studies.[6,7] A value of 0.42 ± 0.05 eV for γ_1 was deduced from a detailed study of the π-band splitting at P,[35] the energy difference $E(P_1^-) - E(P_2^-)$ corresponding to

$4\gamma_1$ in the three-dimensional band structure, Fig. 11.[8] This value is in good agreement with those values determined by recent magnetoreflectance measurements.[36] In the two-dimensional approximation Fig. 4, the separation of the π bands at Q is equal to $2\gamma_b$ so that the thermoreflectance measurements[15] provide a value of approximately 2.4 for γ_0. A simple three-dimensional model[37] gives a value of $2(\gamma_0^2+\gamma_1^2)^{1/2}$ for the π splitting at Q. These values of γ_0 are somewhat lower than currently accepted values determined by Fermi-surface studies, however, probably due to the fact that the Slonczewski-Weiss model[5] is valid only for points very close to the Brillouin-zone edge *HPH*. From the cyclotron-resonance data of Galt, Yager, and Dail[38] it was concluded[6,7] that holes were the carriers at the symmetry point P in the Brillouin zone of graphite, i.e., γ_2 was positive. More recent work[39–42] indicates that γ_2 is negative and that electrons are located at P. While a direct decision on the carrier assignment at P is not possible in the present work, the existence of a strong $\vec{E} \parallel c$ transition, assigned $P_3^- \rightarrow P_3^+$, observed in the SEE spectra, provides strong evidence for P_3^- being located *below* the Fermi level as shown in Fig. 11. That is, the present results indicate electron occupancy at P in agreement with the latest carrier assignment.

IV. CONCLUSIONS

The agreement between the SEE and the PE results, for those $\vec{E} \perp c$ transitions to conduction-band states occurring up to 5 eV above the vacuum level, indicates that excitation with low-energy electrons shows a strong dependence on the same selection rules as those for photon excited transitions. The close correlation between the SEE results and the two-dimensional band structure of Painter and Ellis[3] endorses this view. Indirect processes undoubtedly occur in SEE by incident low-energy electrons, due to momentum transfer to the excited electron. However, as the PE measurements have shown, such processes do not appear to suppress structure due to direct interband transitions.[43] An alternative explanation of the structure observed in the SEE spectrum of graphite in terms of Auger interband transitions[19] cannot account for the positions and intensity variation of the observed maxima. Auger relaxation processes might occur, however; electrons initially excited to conduction-band states could relax into lower band minima by exciting valence electrons to higher states near the Fermi level. Such a mechanism, together with electron-electron and electron-phonon scattering processes, could explain the observed relaxation of electrons into the two minima at Γ and Q in the σ_1 conduction band. The SEE and PE measurements, summarized in Tables I and II, are in good quantitative agreement with transitions predicted within the framework provided by the two-dimensional band structure of Painter and Ellis.[3] However, the present results are not in agreement with their calculation of the structure of the π bands along the three-dimensional Brillouin-zone edge for the multiple-layer graphite lattice in terms of both the magnitude of the splitting and the location of P_3^- relative to the Fermi level. The conclusions regarding the structure of the energy bands may be summarized as follows:

(i) Two minima in the σ_1 conduction band located at critical points Γ_{3u}^+ and Q_{1u}^+ have been observed at 7.5 and 8.6 eV above the Fermi level.

(ii) The σ band gap at the Brillouin-zone center has been measured for $\vec{E} \perp c$ to be 11.5 ± 0.1 eV; the separation of the σ bands increases to 15.0 ± 0.5 eV at Q in good agreement with the optical data[9,12] for transitions assigned $Q_{2g}^+ \rightarrow Q_{1u}^+$.

(iii) An $\vec{E} \parallel c$ transition observed at 14.5 ± 0.5 eV is in good agreement with the predicted value[3] of 13.5 eV assigned to transitions $P_3^- \rightarrow P_3^+$. Emission from final states at Γ_{3u}^+ and Q_{1u}^+ is observed for $\vec{E} \parallel c$ orientation due to the relaxation of electrons initially excited to P_3^+ down into these minima in the σ_1 conduction band.

(iv) Painter and Ellis[3] predict $\vec{E} \parallel c$ transitions at 11 and 16 eV for $P_3^+ \rightarrow P_3^-$ and $Q_{1u}^+ \rightarrow Q_{2g}^-$, respectively, but since both final states are below the vacuum level, these transitions could not be verified directly in the present work. However, the SEE measurements indicate that P_3^- is located *below* the Fermi level which suggests that no transition to this state is possible. This view is endorsed by recent optical reflectivity measurements using a synchrotron source[29] which do not show a strong peak in $\epsilon_{2\parallel}$ at 11 eV, contrary to the analysis of Tosatti and Bassani.[16] The results compiled in Table II locate the initial state Q_{1u}^+ at -12 ± 2 eV below the Fermi level giving a value of 14.5 ± 2 eV for the $Q_{1u}^+ \rightarrow Q_{2g}^-$ transition. The above optical reflectivity measurements[29] and the dielectric constants calculated by Tosatti and Bassani[16] from energy-loss measurements[17] show a weak peak in $\epsilon_{2\parallel}$ around this energy.

Weaker structure at 4.8 and 6.0 eV observed in lower-frequency $\vec{E} \parallel c$ reflectivity measurements[9] cannot be explained in terms of transitions between the highest σ valence band and the lowest π conduction band based on the band structure of Painter and Ellis.[3] However, we point out that transitions between π bands are not strictly forbidden for $\vec{E} \parallel c$ in the three-dimensional model[9] so that this structure could be a consequence of predicted direct transitions at L on the Brillouin-zone face.

(v) The splitting of the π bands at P and Q is observed to be 0.8 eV, which gives rise to $\vec{E} \perp c$ transitions at 4.76 and 4.82 eV associated with the saddle-point nature of the π bands at Q, and a value

0.42 eV for the Slonczewski and Weiss parameter γ_1. These results are in agreement with recent thermoreflectance[15] and magnetoreflectance[36] data.

The SEE measurements locate P_3^- *below* the Fermi level, which provides evidence for electron occupancy at the center of the Brillouin-zone edge, in agreement with recent assignments of electrons rather than holes being located at this point.

To summarize, the combined use of PE and SEE techniques has provided a means of investigating most of the critical points in the band structure of graphite which has in turn served to remove some of the existing discrepancies in the literature regarding the interpretation of the earlier optical data.

ACKNOWLEDGMENTS

We are very grateful to Dr. A. W. Moore of Union Carbide Corp. for supplying samples of highly oriented pyrolytic graphite, and to Dr. M. R. Buyce of the New York State Museum for providing the samples of Ticonderoga graphite. We thank Dr. W. Steinmann, Dr. M. Skibowski, and Dr. R. Klucker of Munich University for informing us of their results prior to publication, and Dr. E. A. Trendelenburg for his advice and encouragement in this study. The skilled assistance of M. Adriaens and D. K. Skinner is gratefully acknowledged.

[1]R. R. Haering and S. Mrozowski, in *Progress in Semiconductors*, edited by A. F. Gibson *et al.* (Heywood and Co. Ltd., London, 1960), Vol. 5, p. 273.

[2]F. Bassani and G. Pastori Parravicini, Nuovo Cimento 50, 95 (1967).

[3]G. S. Painter and D. E. Ellis, Phys. Rev. B 1, 4747 (1970).

[4]W. van Haeringen and H. G. Junginger, Solid State Commun. 7, 1723 (1969).

[5]J. C. Slonczewski and P. R. Weiss, Phys. Rev. 109, 272 (1958).

[6]J. W. McClure, IBM J. Res. Develop. 8, 255 (1964).

[7]M. S. Dresselhaus and J. G. Mavroides, IBM J. Res. Develop. 8, 262 (1964).

[8]E. Doni and G. Pastori Parravicini, Nuovo Cimento 64B, 117 (1969).

[9]D. L. Greenaway, G. Harbeke, F. Bassani, and E. Tosatti, Phys. Rev. 178, 1340 (1969).

[10]F. C. Chalklin, Proc. Roy. Soc. (London) A194, 42 (1948); T. Sagawa, J. Phys. Soc. Japan 21, 49 (1969).

[11]S. Ergun, in *Chemistry and Physics of Carbon*, edited by P. L. Walker, Jr. (Dekker, New York, 1968), Vol. 3, p. 45.

[12]E. A. Taft and H. R. Philipp, Phys. Rev. 138, A197 (1965).

[13]S. Ergun, J. B. Yasinsky, and J. R. Townsend, Carbons 5, 403 (1967).

[14]A. Balzarotti and M. Grandolfo, Phys. Rev. Letters 20, 9 (1968).

[15]M. Anderegg, B. Feuerbacher, and B. Fitton, Phys. Rev. Letters 26, 760 (1971).

[16]E. Tosatti and F. Bassani, Nuovo Cimento, 65B, 161 (1970).

[17]K. Zeppenfeld, Phys. Letters 25A, 335 (1967); Z. Physik 211, 391 (1968).

[18]R. F. Willis, B. Feuerbacher, and B. Fitton, Phys. Letters 34A, 231 (1971).

[19]E. J. Scheibner and L. N. Tharp, Surface Sci. 8, 247 (1967).

[20]R. L. Gerlach, J. E. Houston, and R. L. Park, Appl. Phys. Letters 16, 179 (1970).

[21]C. N. Berglund and W. E. Spicer, Phys. Rev. 136, A1030 (1964).

[22]G. A. Harrower, Phys. Rev. 102, 340 (1956).

[23]B. Feuerbacher and B. Fitton, Rev. Sci. Instr. (to be published).

[24]A. W. Moore, S. L. Strong, and N. F. Greaves, Carbon 7, 714 (1969).

[25]E. G. McRae and C. N. Caldwell, Jr., Surface Sci. 7, 41 (1967).

[26]O. Hachenberg and W. Brauer, Advan. Electron. Electron Phys. 11, 413 (1959).

[27]M. P. Seah, Surface Sci. 17, 132 (1969).

[28]E. Bauer, Z. Physik 224, 19 (1969).

[29]W. Steinmann, M. Skibowski, and R. Klucker (private communication).

[30]E. Taft and L. Apker, Phys. Rev. 99, 1831 (1955).

[31]Physikalisch Technische Bundesanstalt, Braunschweig, Germany.

[32]R. S. Bauer and W. E. Spicer, Bull. Am. Phys. Soc. 15, 386 (1970).

[33]N. V. Smith and M. M. Morton, Phys. Rev. Letters 25, 1017 (1970).

[34]L. D. Laude, B. Fitton, and M. Anderegg, Phys. Rev. Letters 26, 637 (1971).

[35]B. Feuerbacher and B. Fitton, Phys. Rev. Letters 26, 840 (1971).

[36]See, J. A. Woollam [Phys. Rev. Letters 25, 810 (1970)] for a review of recent magnetoreflectance results.

[37]A. Imatake and Y. Uemura, J. Phys. Soc. Japan 28, 410 (1970).

[38]J. K. Galt, W. A. Yager, and H. W. Dail, Jr., Phys. Rev. 103, 1586 (1956).

[39]P. R. Schroeder, M. S. Dresselhaus, and A. Javan, Phys. Rev. Letters 20, 1292 (1968).

[40]J. A. Woollam, Phys. Letters 32A, 115 (1970).

[41]Y. A. Pospelov, Fiz. Tverd. Tela 12, 835 (1970) [Sov. Phys. Solid State 12, 645 (1970)].

[42]I. L. Spain, J. Chem. Phys. 52, 2763 (1970).

[43]Bauer (Ref. 28) has reported fine structure in the energy-loss spectrum of low-energy electrons, 30–300 eV, scattered by silicon surfaces, which can be assigned to direct transitions in agreement with the results obtained with higher-energy 50-KeV electrons (Ref. 44) and the analysis of optical data (Ref. 45).

[44]K. Zeppenfeld and H. Raether, Z. Physik 193, 471 (1966).

[45]R. C. Eden, Stanford University Report No. SU-SEL-67-038, 1967, p. 297 (unpublished).